

Article

Thermodynamic Insights into Sustainable Aviation Fuel Synthesis via CO/CO₂ Hydrogenation

Bin Liang^{1,2}, Qing Zhu³, Zibing Wang⁴, Xiaoyu Fan^{2,5}, Xiao Yu³, Yu Cui⁵, Chenxi Zhang^{1,5,*} and Fei Wei^{1,5}

¹ Beijing Key Laboratory of Green Chemical Reaction Engineering and Technology, Department of Chemical Engineering, Tsinghua University, Beijing 100084, China; lbnn@mail.tsinghua.edu.cn (B.L.); wf-dce@tsinghua.edu.cn (F.W.)

² Institute for Carbon Neutrality, Tsinghua University, Beijing 100084, China; fanxy@mail.tsinghua.edu.cn

³ Institute of Carbon Neutrality, Minzu University of China, Beijing 100081, China; zhuq0008@e.ntu.edu.sg (Q.Z.); yuxiao@muc.edu.cn (X.Y.)

⁴ Tsing Energy Development Hainan Co., Ltd., Haikou 578001, China; luke_manson@163.com

⁵ Ordos Laboratory, Ordos 017010, China; zhihan101@163.com

* Correspondence: cxzhang@mail.tsinghua.edu.cn

Abstract: The transformation of CO/CO₂ hydrogenation into high-density sustainable aviation fuel (SAF) represents a promising pathway for carbon emission reduction in the aviation industry but also serves as a method for renewable energy assimilation. However, current hydrocarbon products synthesized through CO/CO₂ often focus on various catalytic paths with high selectivity and high conversion rates rather than the synthesis of SAFs with complex components. This study undertakes a thermodynamic investigation into the direct or indirect synthesis of SAFs from CO/CO₂ hydrogenation. By analyzing the synthesis of seven aviation fuels defined by the American Society for Testing and Materials (ASTM) D7566 standard, our study reveals a temperature-dependent reduction in the reaction driving force for all products. Specifically, for CO, ΔG transitions from approximately -88.6 J/(mol·K) at 50 °C to 26.7 J/(mol·K) at 500 °C, with the switch from negative to positive values occurring around 390 °C. Similarly, for CO₂, ΔG values change from approximately -66.7 J/(mol·K) at 50 °C to 37.3 J/(mol·K) at 500 °C, with the transition point around 330 °C. The thermodynamic favorability for various hydrocarbon products synthesized is also examined, highlighting a transition at temperatures of around 250 °C, beyond which the thermodynamic drive for the synthesis of aromatic compounds increasingly surpasses that of cycloparaffin synthesis. Our findings also underscore that the products with a higher aromatic content yield a lower H₂/CO₂ ratio, thus reducing hydrogen consumption. The influence of cycloparaffin and aromatic proportions in the typical SAF products on the ΔG is also explored, revealing that an increase in cycloparaffin content in SAFs slightly elevates the ΔG , whereas an increase in aromatic content significantly reduces ΔG , thereby markedly enhancing the thermodynamic drive of the CO/CO₂ hydrogenation reaction. These findings underscore the thermodynamic preference for synthesizing SAF with a higher proportion of aromatic compounds, shedding light on potential pathways for optimizing fuel synthesis to improve efficiency. Finally, the thermodynamic challenges and potential solutions involved in synthesizing SAFs via specific intermediate compounds are discussed, presenting opportunities for more strategic process schemes in industrial scenarios.

Keywords: sustainable aviation fuel; CO/CO₂ hydrogenation; thermodynamic; reaction driving force; intermediate compounds



Citation: Liang, B.; Zhu, Q.; Wang, Z.; Fan, X.; Yu, X.; Cui, Y.; Zhang, C.; Wei, F. Thermodynamic Insights into Sustainable Aviation Fuel Synthesis via CO/CO₂ Hydrogenation. *Catalysts* **2023**, *13*, 1396. <https://doi.org/10.3390/catal13111396>

Academic Editor: Zhong-Wen Liu

Received: 27 August 2023

Revised: 19 October 2023

Accepted: 23 October 2023

Published: 26 October 2023



Copyright: © 2023 by the authors. Licensee MDPI, Basel, Switzerland. This article is an open access article distributed under the terms and conditions of the Creative Commons Attribution (CC BY) license (<https://creativecommons.org/licenses/by/4.0/>).

1. Introduction

In recent years, CO₂ emissions from traditional fossil fuels have escalated, causing considerable environmental concerns [1]. Under the background of “carbon neutrality”, The aviation industry, accounting for 2~3% of global CO₂ emissions, is under pressure to

adapt in the era of “carbon neutrality [2]”. With the sustained growth of the global economy and increasing international cooperation, CO₂ emissions from the aviation industry will continue to rise [3]. Meanwhile, the swift electrification of aviation is hampered by the vast energy density difference between liquid hydrocarbon aviation fuels and commercial lithium–ion batteries, emphasizing the need for carbon-neutral alternatives [4–6].

1.1. Development of Bio-Based Sustainable Aviation Fuels

Green aviation fuels, especially Sustainable Aviation Fuels (SAFs), have emerged as potential remedies. SAFs can notably reduce the aviation industry’s carbon footprint. There are four main pathways for SAF production: Hydro-processed Esters and Fatty Acids (HEFA), Gas + Fischer–Tropsch (G + FT), Alcohol to Jet (AtJ), and Power to Liquid (PtL). According to the European Union Aviation Safety Agency (EASA), HEFA is the most commercially mature, with others still in varying stages of development.

The latest ASTM (American Society for Testing and Materials) D7566-22a standard highlights seven biomass-derived components for jet fuel, expanding potential biomass-based jet fuel sources. These components include Fischer–Tropsch Synthetic Paraffinic Kerosene (FT-SPK), Hydro-processed Esters and Fatty Acids Synthetic Paraffinic Kerosene (HEFA-SPK), Synthetic Isoparaffin (SIP) derived from sugar fermentation products, Aromatic-containing Fischer–Tropsch Synthetic Paraffinic Kerosene (FT-SPK/A), Alcohol to Jet Synthetic Paraffinic Kerosene (ATJ-SPK) synthesized predominantly from ethanol and isobutanol, Catalytic Hydrothermolysis Jet Synthetic Paraffinic Kerosene (CHJ-SPK) produced through the catalytic pyrolysis of oil fats, and Hydro-processed Cyclic Hydrocarbon Hydro-processed Esters and Fatty Acids Synthetic Paraffinic Kerosene (HC-HEFA-SPK). According to the lifecycle analysis conducted by UOP (Universal Oil Products), the bio-jet fuel produced through this process demonstrated a reduction in greenhouse gas emissions ranging from 65% to 85% compared to petroleum-based jet fuel.

However, almost all SAF technologies have certain limitations compared to conventional fossil-based jet fuels. It is worth noting that this process has a high hydrogen consumption rate, which can increase production costs and pose safety concerns in the manufacturing process [7]. The production process of FT bio-jet fuel is indeed complex and costly, while also exhibiting relatively lower process efficiency. Additionally, due to the absence of aromatics that are controlled by Anderson–Schulz–Flory (ASF) distribution [8], FT bio-jet fuel has a lower energy density, resulting in reduced power output and lower fuel economy [9]. In addition, aromatics are important for fuel lubricity and rubber compatibility.

1.2. An Overview of CO/CO₂ Catalytic Hydrogenation to Aviation Fuel Components

Countries like China face additional hurdles due to the scattered distribution of biomass resources, cost implications, and potential conflicts between food production and biomass for fuel [10,11]. Although SAF from biomass is advancing, commercial viability is not yet solidified [12]. The cost of biomass conversion to SAF typically surpasses that of extracting aviation fuels from petroleum, primarily due to the complexity of the conversion process, lower energy efficiency, and higher costs of biomass collection and transportation [13]. Even though biomass is renewable, improper management, such as overexploitation and irrational land use, could result in biodiversity loss, soil erosion, water contamination, and other environmental concerns.

Given these challenges, the catalytic hydrogenation of CO/CO₂ presents a promising alternative for green aviation fuel production. CO₂ can serve as a carbon source, reacting with hydrogen produced from renewable energy sources, such as solar power, wind energy, and biomass energy, to create high-value chemicals [14,15]. To date, the majority of research has been directed towards hydrogenating CO₂ to produce short-chain products, such as methane [16,17], methanol [18,19], formic acid [20,21], dimethyl ether [22,23], and low-carbon olefins [24]. Conversely, less attention has been devoted to the synthesis of long-chain products from CO₂ [25].

Furthermore, the conversion of CO₂ to aromatics through hydrogenation represents a significant challenge due to the thermodynamic stability and chemical inertness of CO₂ and the kinetic barriers associated with C–C bond formation [26]. It is worth noting, however, that carbon monoxide (CO), as the “twin brother” of CO₂, is relatively easier to activate. Additionally, synthesis gas (CO/H₂) can be obtained from non-petroleum carbon resources [27]. CO₂ can also be converted into synthesis gas through the reverse water gas shift reaction (RWGS) [28]. However, the conventional F-T synthesis is subject to the ASF distribution, which makes the control over product distribution challenging [8]. Therefore, it necessitates the development of an efficient and stable catalyst to overcome the product limitations imposed by the ASF distribution.

In 1979, Chang et al. first proposed the use of a novel catalyst combining a metal (Fe, Zr, Zn–Cr) with CO reduction capability and HZSM-5 zeolite [29]. This combination disrupted the ASF distribution, diminished the selectivity for linear hydrocarbons, and significantly elevated the selectivity for aromatics. Recently, composite catalysts (metal–metal/oxide/zeolite) have become one of the research hotspots in C1 chemistry. This reaction coupling strategy is also applicable to the direct conversion of CO₂ to aromatics [30]. A composite catalyst refers to a catalyst with multiple active sites, coupling and catalyzing sequential reactions. In this context, the types of intermediates formed between consecutive reactions play a decisive role in product distribution. These intermediates can be directly transferred to the active sites of the subsequent reaction, enabling the second reaction to consume the products of the first. This action, in turn, drives the equilibrium of the initial reaction forward, following Le Chatelier’s principle [31,32].

The formation of intermediates in the catalytic hydrogenation of CO/CO₂ significantly varies with factors such as the type of catalyst, reaction conditions, reactor type, reaction time, and the medium in which the reaction takes place. Common intermediates, subject to these variables, include methanol [33], ketene [34], formaldehyde [35], ethylene [36], hexene [37], dimethyl ether (ethanol) [38], methoxyphenol [39], and formic acid [40]. However, these factors are governed by kinetics, while the potential for the intermediates to form during the CO/CO₂ hydrogenation reaction, and their ultimate transformation into the desired products, is determined by the change in Gibbs free energy before and after the reaction under thermodynamic considerations.

Despite considerable research efforts dedicated to the high-selectivity transformation of CO/CO₂ to specific hydrocarbon target products through specific intermediates, there remains a noticeable gap in thermodynamic investigations specifically aimed at the seven synthetic hydrocarbon compounds listed in standard D7566 for aviation turbine fuel. This gap is of significant importance for the selection of reaction pathways and the synthesis of catalysts.

1.3. The Objectives of This Study

Therefore, this study primarily focuses on assessing the thermodynamic feasibility of directly or indirectly synthesizing the seven aviation turbine fuels specified in the ASTM D7566 standard through the hydrogenation of CO/CO₂. Initially, we conduct a comparative analysis of the thermodynamic driving forces involved in synthesizing varying types of hydrocarbons (cycloparaffins, aromatics, and paraffins). This is followed by an evaluation of how the carbon number, as well as the proportion of cycloparaffins and aromatics in the products, impacts the thermodynamic driving force. Additionally, we present an argument for the most appropriate hydrocarbon targets in the production of SAF via the CO/CO₂ hydrogenation process, taking into account both thermodynamic preferences and hydrogen consumption. Subsequently, we delve into the practicality of obtaining aviation fuel products via different reaction pathways (that is, with different intermediates) in CO/CO₂ hydrogenation. Finally, we provide a brief review of our recent research progress on the catalysts and catalytic mechanisms involved in the one-step hydrogenation of CO/CO₂ to different hydrocarbon products. These results will guide the development of process routes for the high-selectivity direct conversion of CO/CO₂ into green aviation fuels.

2. Results and Discussion

2.1. Direct Synthesis of SAF via CO/CO₂ Hydrogenation

To initiate our investigation, we conducted a thermodynamic analysis of the direct synthesis of the seven aviation fuels, as specified in the ASTM D7566 standard, through CO/CO₂ hydrogenation. From the perspective of oxygen balancing, CO/CO₂ hydrogenation can lead to two equilibriums: one yielding H₂O, and another producing CO₂ (using CO hydrogenation as an illustration). Both of these are alongside aviation fuel blends. Consequently, we primarily compared the thermodynamic parameters of these two pathways. Figure 1 reveals that for both routes, ΔG increases with temperature, with spontaneity maintained below 400 °C ($\Delta G < 0$). Importantly, the H₂O-yielding route consistently shows a more favorable ΔG . Industrially, this route is advantageous, avoiding additional greenhouse gas (CO₂) emissions or the waste of valuable gases, like CO formed during CO₂ hydrogenation. In light of these findings, all ensuing thermodynamic evaluations in this study are based on equations balanced with H₂O as the product.

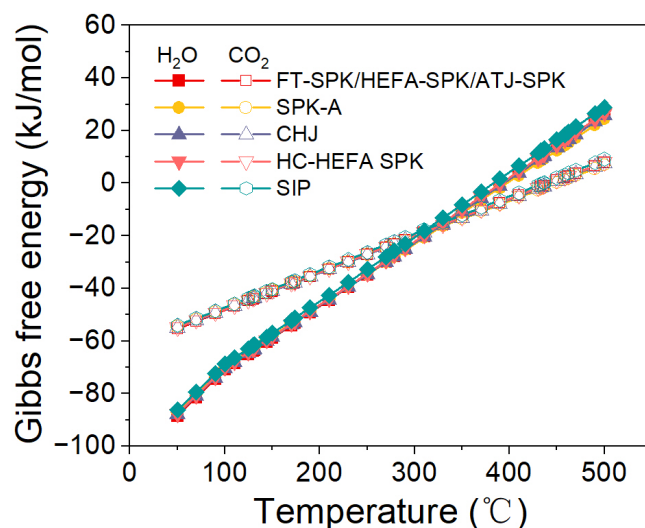


Figure 1. Comparison of ΔG as a function of temperature for CO hydrogenation with H₂O and CO₂ as products.

Figure 2 shows the temperature-dependent variation of ΔG in the conversion pathway from CO/CO₂ to various SAFs. It also illustrates an increase in ΔG values of all products as the temperature rises, indicating a reduction in the driving force of the reaction at elevated temperatures. This trend is attributed to the exothermic nature of the CO/CO₂ hydrogenation process. Notably, due to the inherent chemical inertness and thermodynamic stability of CO₂, the temperature-dependent ΔG curve for CO₂ hydrogenation consistently positions itself above that of the CO hydrogenation. However, the difference in ΔG between the hydrogenation processes of CO and CO₂ narrows as the temperature elevates. It can be attributed to both the differential entropy values of the two substances and their respective activation processes. Structurally, CO₂ is more symmetrical than CO, leading to distinct entropy values (197.7 J/(mol·K) for CO and 213.6 J/(mol·K) for CO₂ under standard conditions). In hydrogenation reactions, the entropy change (ΔS) predominantly arises from the reactants rather than products. As temperature rises, as can be shown in Equation (1), the smaller entropy of CO yields a reduced $T\Delta S$ term for its hydrogenation, narrowing the ΔG difference.

$$\Delta G = \Delta H - T\Delta S \quad (1)$$

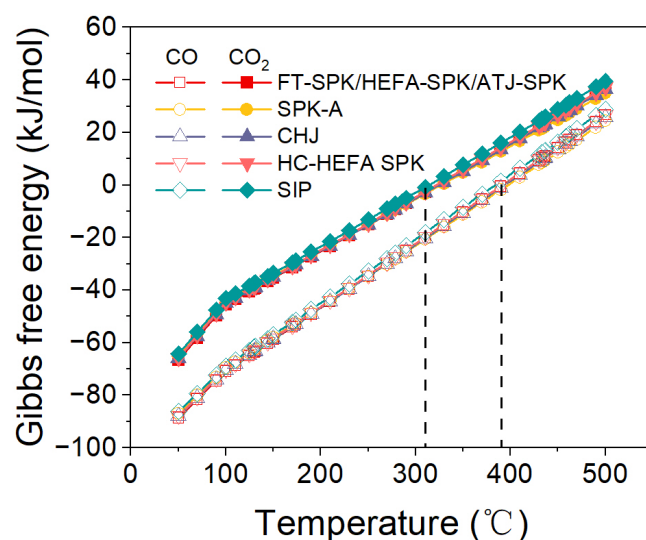


Figure 2. Temperature-dependent variation of ΔG in the conversion pathway from CO/CO₂ to SAF.

Additionally, elevated temperatures facilitate the activation of the chemically inert CO₂, enhancing its reactivity with hydrogen. Conversely, CO's lower activation energy makes it less temperature-sensitive, implying a faster relative reaction rate increase for CO₂ hydrogenation as temperatures escalate, further contracting the ΔG gap between them.

Regarding the hydrogenation reactions of CO and CO₂, the transition of ΔG from negative to positive occurs at approximately 390 °C and 330 °C, respectively. Beyond these temperatures, the reactions are not spontaneously feasible. These findings play a pivotal role in determining the optimal reaction temperatures. In practice, under pressurized conditions, hydrocarbon synthesis through CO and CO₂ hydrogenation typically occurs below 400 °C [36,41–44] and 350 °C [45–47], respectively. These results demonstrate that under appropriate reaction conditions, there exists the potential to directly synthesize SAF products that meet standard requirements through the hydrogenation of CO and CO₂.

Upon further comparing the thermodynamic driving forces for different hydrocarbon products during the CO/CO₂ hydrogenation process, as illustrated in Figure 3, it is evident that for both CO and CO₂ hydrogenation, when the temperature is below 250 °C, the absolute value of ΔG for paraffin products is higher than that for cycloparaffins and aromatics when synthesizing hydrocarbon components with the same carbon number. Nonetheless, as the temperature ascends, the thermodynamic driving force of CO/CO₂ hydrogenation towards aromatics progressively amplifies. This observation can be further corroborated by the data presented in Figures 4 and 5, which demonstrate the comparison of ΔG for three hydrocarbon components during the CO/CO₂ hydrogenation reaction at two specific temperatures. The results indicate that the discrepancy in the absolute values of ΔG for aromatic hydrocarbons and the other two hydrocarbon components is considerably larger at higher temperatures than at lower ones, suggesting that a noticeably stronger thermodynamic drive for the synthesis of aromatics from CO/CO₂ hydrogenation. Our research group has previously reported that high selectivity for mononuclear aromatic hydrocarbon products (C8–C12) can be achieved via the single-pass conversion of CO or CO₂ on a physically mixed nanoscale composite catalyst composed of ZnCr₂O₄ (with a Zn/Cr ratio of 0.54) and Sbx-HZSM-5. This can be attributed to the thermodynamically controlled CO/CO₂ hydrogenation process, which significantly enhances the capability of synthesizing high-value aromatic hydrocarbons [48].

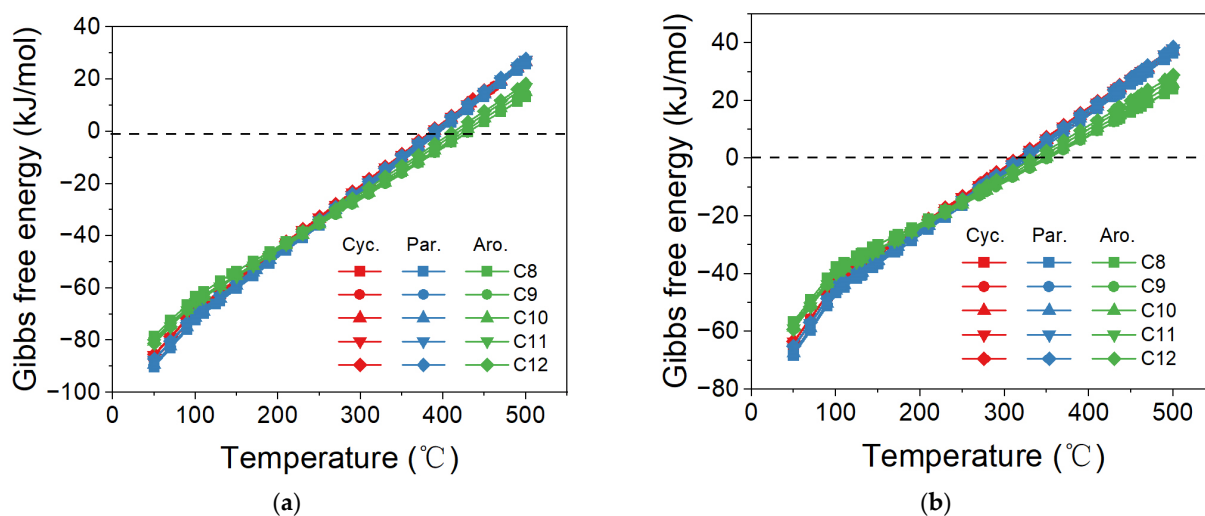


Figure 3. Temperature-dependent variation of ΔG for the synthesis of different hydrocarbon components from CO/CO₂. (a) CO. (b) CO₂.

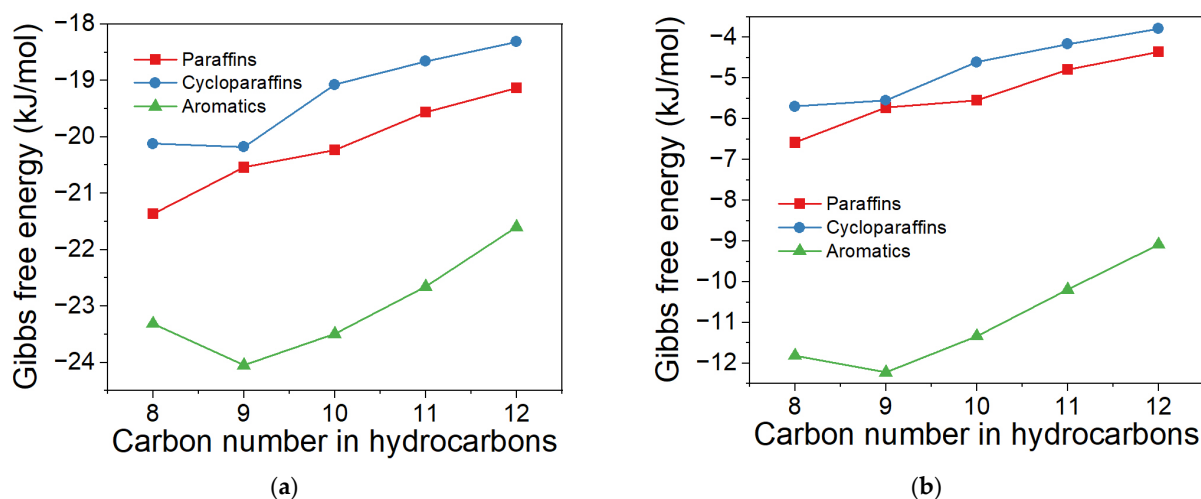


Figure 4. Effect of carbon number in products on ΔG for CO hydrogenation under different temperatures. (a) 310 °C. (b) 370 °C.

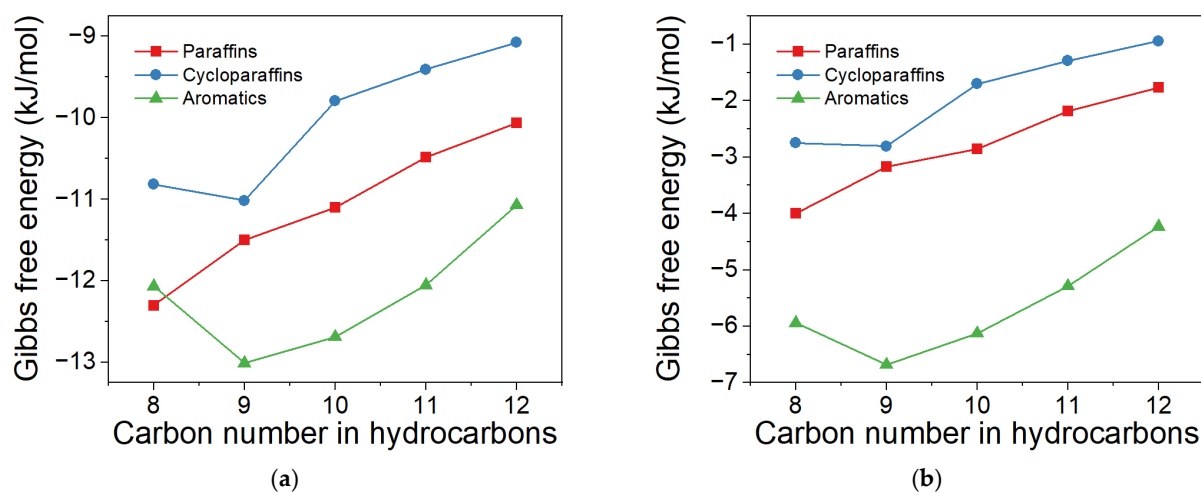


Figure 5. Effect of carbon number in products on ΔG for CO₂ hydrogenation under different temperatures. (a) 270 °C. (b) 310 °C.

Contrary to CO hydrogenation, CO₂ hydrogenation goes through an RWGS reaction (Equation (2)), resulting in H₂O and CO as the primary by-products.



On the one hand, the RWGS reaction can reduce CO₂ to the more reactive CO, which is beneficial for the progress of the hydrogenation reaction [49]. On the other hand, the RWGS reaction is endothermic, which competes with the formation of aviation fuel components at higher temperatures [50]. As illustrated in Figure 6, the temperature at which the RWGS reaction spontaneously occurs at atmospheric pressure is generally above 800 °C. However, the catalytic hydrogenation reaction of CO/CO₂ is usually conducted under high pressure, at which point the temperature required for the spontaneous occurrence of the RWGS reaction drops below 400 °C, directly competing with the production of aviation fuel components. Ni et al. (2018) conducted CO₂ hydrogenation on a composite catalyst composed of nano-spinel-structured ZnAlO_x and HZSM-5. They found that increasing the H₂/CO₂ feed ratio or introducing CO could effectively inhibit the RWGS reaction, thereby reducing the formation of by-products [35].

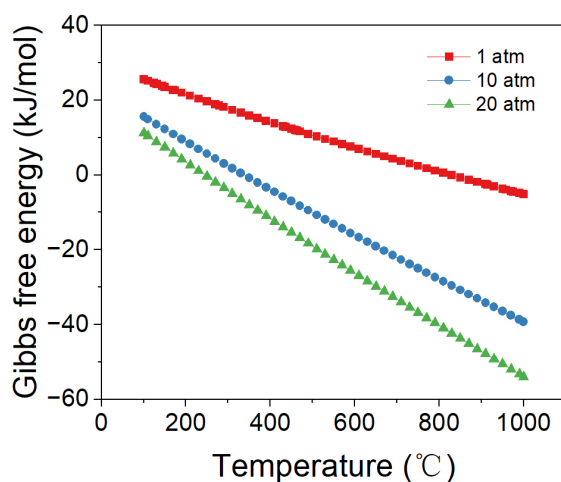


Figure 6. Effect of pressure and temperature on ΔG for RWGS reaction.

2.2. Effect of Proportions of Cycloparaffin and Aromatic in Products on ΔG

High-density fuels are pivotal to the future of SAF, contributing to the miniaturization of aircraft, and enhancing their flexibility. Notably, increasing the proportion of polycyclic hydrocarbons in fuel significantly boosts its energy density. Given this, a thorough understanding of the impact of cycloparaffin and aromatic compositions in SAFs derived from CO/CO₂ hydrogenation on the ΔG is crucial for optimizing fuel synthesis and achieving maximum efficiency. Accordingly, we selected two representative products, FT-SPK and SPK/A, to study the influence of the proportion of cycloparaffin in FT-SPK and that of the aromatics in SPK/A on the ΔG . FT-SPK, the earliest aviation fuel listed in the ASTM D7566 standard, contains a substantial amount of n-alkanes, iso-alkanes, and a limited quantity of cycloparaffins (less than 15% by mass). It exhibits a lower density with negligible traces of heteroatom compounds and aromatics hydrocarbons [51]. The composition is similar to that of HEFA-SPK and ATJ-SPK, making it a suitable subject for studying the impact of cycloparaffin proportion on ΔG . Considering the significance of energy density and lubricity in aviation fuel properties, the ASTM standard allows for up to 20% by mass of aromatic components in SPK/A. Given that the SPK/A composition encompasses that of CHJ, it serves as an appropriate selection for examining the effect of aromatic ratios on the ΔG .

As depicted in Figure 7, under reaction conditions of 310 °C and atmospheric pressure (where ΔG is close to zero), the ΔG in the CO/CO₂ hydrogenation process exhibits contrasting trends with the increased proportions of cycloparaffin and aromatic compounds in

their respective products (FT-SPK and SPK/A). Specifically, an increase in the cycloparaffin content in FT-SPK slightly enhances the ΔG . For instance, in the CO_2 hydrogenation process, as the proportion of cycloparaffins in the product rises from 0% to 16%, ΔG shifts from $-2.9 \text{ J}/(\text{mol}\cdot\text{K})$ to $-2.7 \text{ J}/(\text{mol}\cdot\text{K})$. Conversely, for SPK/A, an enhancement in the aromatic content notably diminishes ΔG , transitioning from $-2.7 \text{ J}/(\text{mol}\cdot\text{K})$ to $-3.3 \text{ J}/(\text{mol}\cdot\text{K})$ as the aromatic concentration increases from 0% to 20%. This underlines that the enrichment of aromatics in SAF products amplifies the driving force of the CO/CO_2 hydrogenation reaction. Moreover, under identical reaction conditions, the absolute values of ΔG for SPK/A are considerably lower than that for FT-SPK. These results corroborate that thermodynamically, it is more feasible to have aromatics as the major product constituents than cycloparaffins.

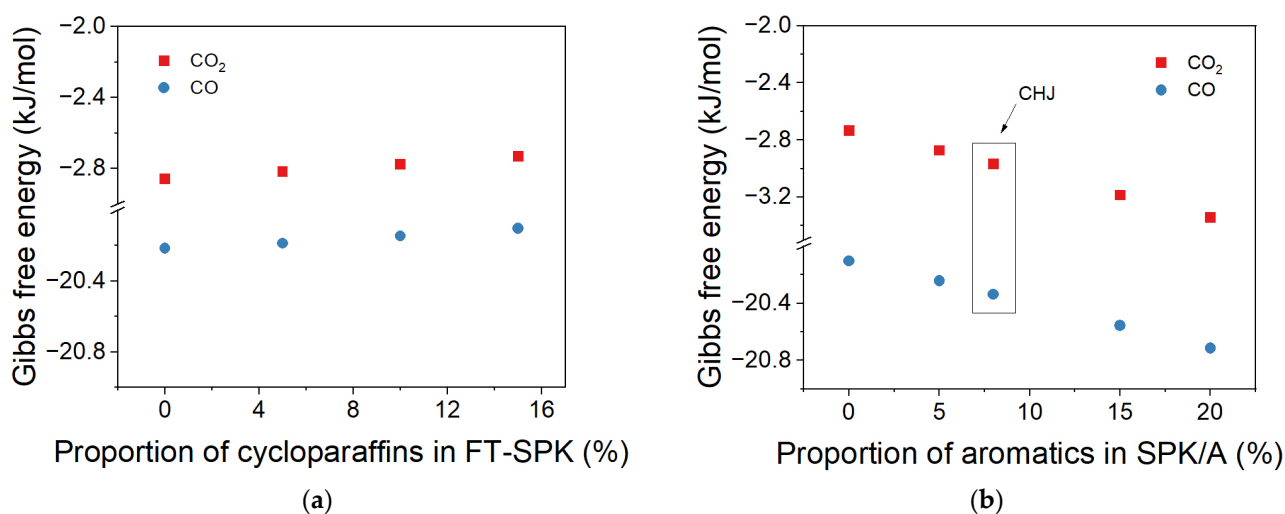


Figure 7. The effect of the proportion of cycloparaffins and aromatics in products on ΔG (310°C). (a) Cycloparaffins in FT-SPK. (b) Aromatics in SPK/A.

Further, by balancing the hydrogenation process, we obtained the molar ratio of H/C for different target products. Given the consistency of the H/C trends irrespective of whether CO or CO_2 hydrogenation was performed, we use CO_2 hydrogenation as an example in this article (Figure 8). As can be clearly seen from Figure 8a, SPK/A, the product with the highest aromatic content, has the lowest H_2/CO_2 . This further demonstrates that the synthetic pathway with aromatics as the product has the lowest hydrogen consumption. The results in Figure 8b further confirm this conclusion. The H_2/CO_2 ratio of the conversion process targeting aromatics as the product is significantly lower than that targeting cycloparaffins. In addition, in contrast to the unclear change in H_2/CO_2 ratio with the increase in the proportion of cycloparaffins, the value of H_2/CO_2 significantly decreases with the increase in the content of aromatics in the product. This underscores the thermodynamic advantage of targeting aromatics, which simultaneously ensures reduced hydrogen consumption among hydrocarbon compounds. Given the imperative for enhanced jet fuel performance in future aircrafts, the role of aromatics in aviation fuel is indisputable [48,52]. Beyond augmenting energy density—a critical factor for extended flights—aromatics play a pivotal role in enhancing fuel lubricity, thereby safeguarding engine components. Recognizing these advantages, combined with reduced hydrogen consumption in their synthesis, it is evident that SAF strategies should emphasize CO/CO_2 conversion pathways with elevated aromatic yields. Such an approach not only addresses thermodynamic efficiency but also aligns with practical aviation fuel specifications.

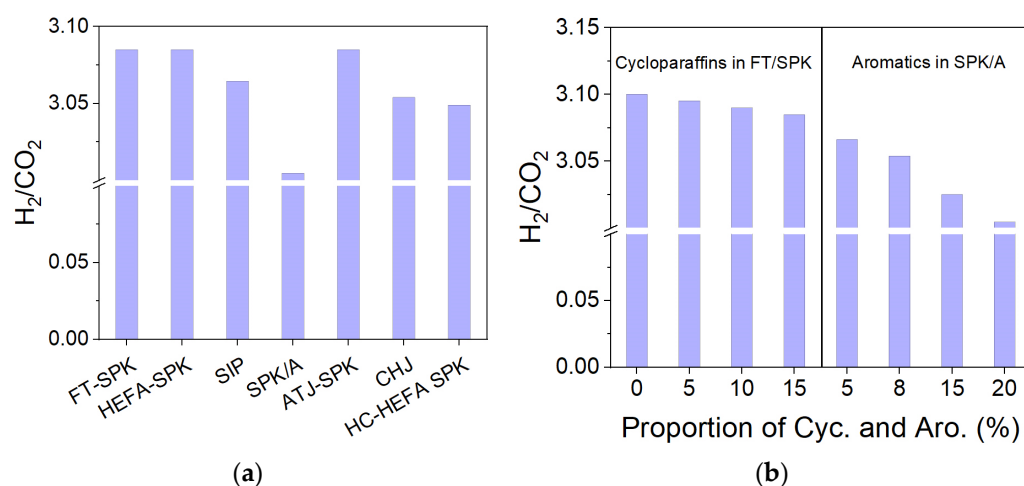


Figure 8. The effect of hydrocarbon types in the products on the H₂/CO₂. (a) Seven SAF products. (b) Products with different cycloparaffins and aromatics proportions.

2.3. Reaction Pathways for SAF Synthesis via CO/CO₂ Hydrogenation

While direct synthesis offers a pathway for CO/CO₂ hydrogenation to targeted hydrocarbons [53], an alternative, often-employed strategy involves a two-step indirect method [54,55], wherein CO/CO₂ is first transformed into intermediate compounds, which subsequently undergo conversion to yield the desired hydrocarbons. The key to achieving high selectivity in the synthesis of target products lies in the thermodynamic and kinetic coordination of multiple reactions [56]. Consequently, our first step was to calculate the variation in the ΔG with temperature for the CO/CO₂ hydrogenation to common precursor compounds, which can be seen in Figure 9. The ΔG for all the reaction processes shows an increasing trend with the temperature rise, indicating that the CO/CO₂ hydrogenation to form intermediate compounds is exothermic. Also, the variation curve of ΔG with temperature for CO₂ always lies above that for CO. However, the conditions for spontaneous reactions involving methanol, ketene, formaldehyde and formic acid as intermediates seem rather stringent, requiring lower temperatures to proceed. Meanwhile, other intermediates, including ethene, hexene, ethanol (dimethyl ether), and methylphenol, retain a ΔG less than zero at approximately 300 °C. It is worth noting that reactions involving carbon–carbon (C–C) coupling typically exhibit stronger thermodynamic driving forces compared to those without C–C coupling.

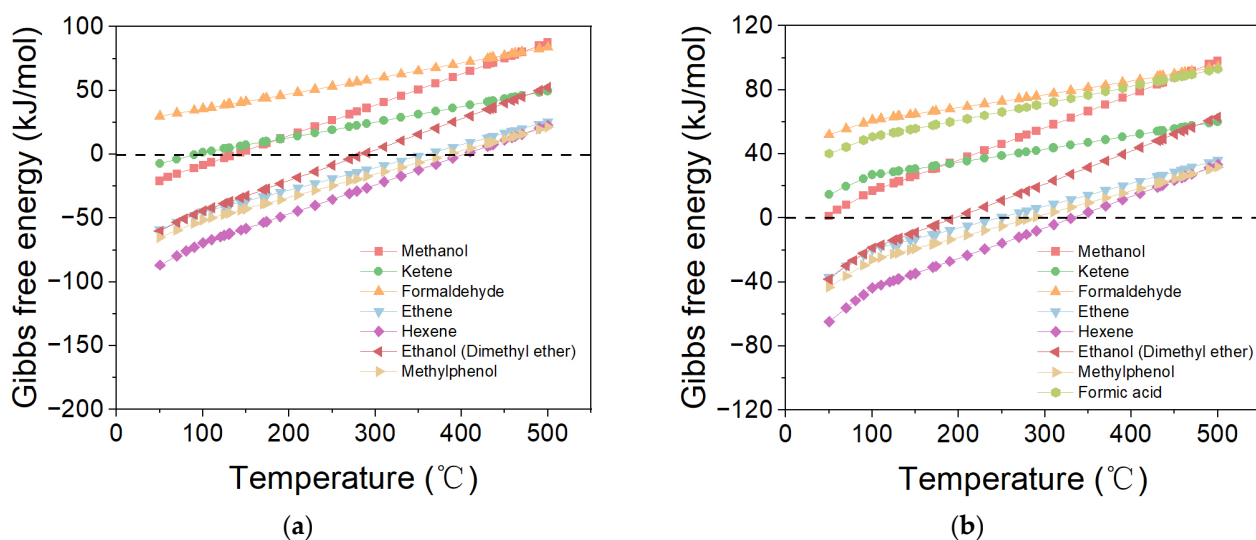


Figure 9. Temperature-dependent variation of ΔG in the conversion pathway from CO/CO₂ to specific intermediates. (a) CO. (b) CO₂.

However, thermodynamic constraints further complicate the conversion of certain spontaneously obtained intermediate compounds from CO/CO₂ hydrogenation into aviation fuel products. Given that the ΔG trends for pathways such as FT-SPK, SIP, SPK/A, and HC-HEFA SPK are notably analogous with only slight differences in exact ΔG values, we chose to exemplify this using the FT-SPK pathway in Figure 10. As shown in Figure 10, the transformation of hexene into different aviation fuel products can no longer spontaneously occur at around 50 °C, and the ΔG for the conversion of ethene and methanol turns from negative to positive at higher reaction temperatures. However, the transformation of intermediate compounds, such as methanol, ketene, and formaldehyde, into different aviation fuels exhibits a strong thermodynamic driving force. In particular for methanol, its transformation process displays minimal dependency on the reaction temperature in terms of its ΔG change. Thus, thermodynamically, the subsequent conversion of methanol to aviation fuels can promote the initial step of transforming CO/CO₂ into aviation fuels. In summary, the thermodynamic feasibility of synthesizing aviation fuels via the indirect method of CO/CO₂ hydrogenation depends on selecting reaction pathways where both steps exhibit negative Gibbs free energy changes under suitable reaction conditions. This ensures that the thermodynamic driving force acts favorably to promote both steps of the reactions. These results enable an optional range of coupling temperature zones for various reaction pathways, offering strategic insights for process schemes in actual industrial scenarios.

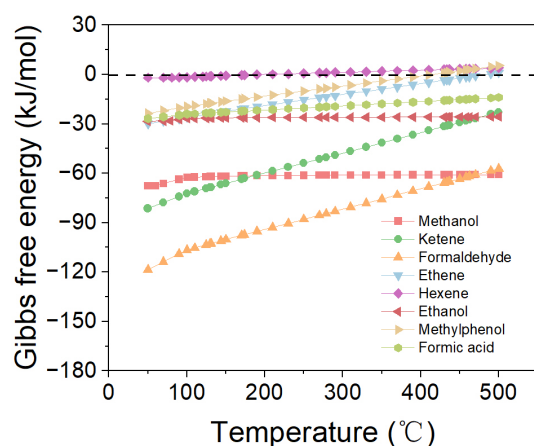


Figure 10. Temperature-dependent variation of ΔG in the conversion pathway from specific intermediates to SAF.

2.4. Direct CO/CO₂ Hydrogenation to Aromatics: Our Recent Research and Catalytic Strategies

The increasing demand for high-density SAFs, coupled with the thermodynamic and environmental advantages of using CO/CO₂ as feedstocks, has steered significant research attention towards the direct hydrogenation of these compounds, to synthesize aromatics, pivotal precursors for the kerosene-based aviation fuel. While synthesis-gas-derived routes to aromatics, such as the conversion from synthesis gas to methanol followed by its subsequent transformation to aromatics (MTA), have been well established, the direct one-step conversion of CO/CO₂ to aromatics offers notable advantages. By circumventing intermediate steps, the direct approach promises potential reductions in energy consumption and, when coupled with apt catalyst selection, can achieve desirable product yields and selectivity.

To further guide the design of catalysts for the hydrogenation of CO/CO₂ to aromatics and elucidate the mechanisms of the catalytic reaction, our research group has embarked on extensive studies. A significant challenge encountered in this domain is the control of selectivity during the single-step conversion of syngas to single aromatic hydrocarbon, with an emphasis on enhancing CO utilization [57]. A breakthrough was achieved using the reaction coupling methodology, facilitating a high selectivity of approximately 70% for a single product, tetramethylbenzene (TeMB), at a total CO conversion of 37%. This

feat was realized by employing H₂-deficient syngas over a composite catalyst comprising nanosized ZnCr₂O₄ and HZSM-5. Unique channeling in the HZSM-5 catalyst played a pivotal role in achieving high selectivity for aromatics. The dual-cycle mechanism was skewed towards aromatics due to enhanced molecular diffusion and selective methanol formation, resulting in dominant aromatic cycles.

In response to global carbon concerns and the European Union's aviation carbon tax (ACT), our team pioneered a carbon-neutral strategy to synthesize precursors, such as aromatics, alkyl benzenes, and naphthenes, from waste CO₂ or biomass-derived syngas [48]. These precursors form a significant portion of kerosene-based aviation fuel. Remarkably, an ultra-high selectivity (>80% in hydrocarbons) for single-ring aromatics within the C₈–C₁₂ range was observed at a reaction temperature of 275 °C. The formation of these aromatics was rooted in an "aldol-aromatic" mechanism. In addition to thermodynamics, the catalyst topology and the presence of highly active oxygenated species in the hydrocarbon pool were attributed to the heightened selectivity.

A deeper dive into the reaction mechanism revealed the emergence of an aldol-aromatic pathway, consisting of aldol, phenolic, and aromatic cycles [39]. This mechanism enabled >70% selectivity for TeMB in hydrocarbons at a mere 275 °C. The proximity of ZnCr₂O₄ and HZSM-5 catalytic sites bolstered the formation of aromatics, underscoring the pivotal role of oxygenated-aromatic compounds in the carbon pool. The process efficiency was enhanced due to thermodynamic equilibrium, surface methylation, and static repulsion. Our group also penned a mini-review that shed light on the intricate mechanisms underpinning the conversion of CO_x into valuable green aromatics [53]. Emphasis was placed on the nano-scale intricacies, elucidating factors like the proximity of active sites and overall thermodynamic analysis.

Building on these insights, the introduction of monodispersed Fe on ZnCr₂O₄, when paired with HZSM-5 zeolite, showcased exceptional performance in the syngas-to-aromatic reaction [31]. With this innovation, the turnover frequency surged to 0.48 s⁻¹, while maintaining an impressive aromatic selectivity between 80 and 90%. This elevation in activity was ascribed to efficient CO and H₂ activation, underpinned by the prevention of carbide formation.

Lastly, in a recent perspective, the promise of CO_x hydrogenation for sustainable chemical production was reiterated [30]. Heterogeneous catalytic CO_x hydrogenation to high-carbon-number products (C₈+) showcased the potential, especially when deploying tandem catalysts composed of metal oxides and nano-porous zeolites. The spotlight was on understanding reaction mechanisms and identifying speciation-sensitive activity descriptors, emphasizing H* adsorption energy and zeolite topologies. These insights can underpin the future design of high-performing catalysts for CO_x hydrogenation to aromatics.

In light of the aforementioned discussion on the thermodynamic exploration of CO/CO₂ hydrogenation for SAF synthesis and our research group's unwavering dedication to unravel the catalytic systems for CO/CO₂ hydrogenation into aromatics, we aspire to pave a promising pathway for the future. Our endeavors emphasize the potential of a direct one-step catalytic hydrogenation of CO/CO₂ for SAF synthesis. Through rigorous investigation and innovative approaches, we aim to provide an alternative and sustainable route for aviation fuel production, leveraging the carbon-neutral capabilities and high selectivity attributes of our devised catalytic systems. This trajectory not only addresses environmental imperatives but also heralds a revolutionary step in aviation fuel synthesis, amplifying the feasibility and desirability of transitioning to greener alternatives in the aviation sector.

3. Methodology

The thermodynamic software package Factsage (Ver. 8.2, GTT Technologies, Herzogenrath, Germany, 2022) with the database of FToxid, which is built on the foundation of Gibbs' energy minimization principle, was used in this study to calculate ΔG values for the reactions involving CO/CO₂ and H₂. Beyond the calculated temperature range for

the reverse water gas shift reaction (RWGS, 50 °C~1000 °C), all calculations were carried out over a temperature ranging from 50 °C to 500 °C, with an interval of 20 °C, under atmospheric pressure.

Prior to the thermodynamic calculations for the bio-based SAF production via CO/CO₂ hydrogenation synthesis, it is critical to first ascertain the production composition. This information enables the balancing of the stoichiometric coefficients of the reactants and products in the chemical equations. Drawing from the insights gleaned from literature reports and our research team's preliminary findings [13,48], we have established that the aviation fuel composition primarily encompasses hydrocarbons from C₈ to C₁₂. In terms of the total mass fraction of the products, C₈, C₁₁, and C₁₂ each constitute 10%, while C₉ and C₁₀ each account for 35%.

Building upon the ASTM D7566 standard, our breakdown of the seven SAF products (refer to Table 1) primarily features paraffins, cycloparaffins, and aromatics. The standard offers clear guidelines regarding the proportions of these hydrocarbon groups in each SAF product. With this foundation, we have detailed the specific hydrocarbons, spanning from C₈H₁₈ to C₁₂H₂₆ for paraffins, C₈H₁₆ to C₁₂H₂₄ for cycloparaffins, and C₈H₁₀ to C₁₂H₁₈ for aromatics. Their specific ratios in each SAF product were also determined. For SIP products, primarily composed of farnesane and hexahydrofarnesol, our breakdown constitutes 97% of C₁₅H₃₂ and 1.5% of C₁₅H₃₂O, with the remaining 1.5% as paraffins.

Table 1. Composition of hydrocarbon compounds in the aviation turbine fuel as per ASTM D7566 standard.

Standard	FT-SPK	HEFA-SPK	SIP	SPK/A	ATJ-SPK	CHJ	HC-HEFA SPK
Hydrocarbon Composition							
Saturated Hydrocarbons, %			98				
Farnesane, %			97				
Hexahydrofarnesol, %			1.5				
Olefins, mgBr ₂ /100 g			300				
Cycloparaffins, %	15	15		15	15	report	50
Aromatics, %	0.5	0.5	0.5	20	0.5	8.4~21.2	0.5
Paraffins, %	report	report			report	report	report
Carbon and Hydrogen, %	99.5	99.5	99.5	99.5	99.5		99.5

Once these compositions were established, the subsequent step was to balance the chemical equations that describe the reactions of CO/CO₂ with H₂ to produce these SAF constituents. However, given that the balanced chemical equations will yield different stoichiometric quantities of CO/CO₂ reactants based on the various compositions of the products, this will result in variations in the ΔG. Therefore, in this study, all data processing is conducted in terms of the ΔG per mole of carbon to normalize the analysis results.

To further investigate how the contents of cycloparaffins and aromatics in SAFs influence thermodynamic behavior during CO/CO₂ hydrogenation, we adjusted their levels in both FT-SPK and SPK/A SAF types. Concurrently, we modified the paraffin content to ensure that the cumulative percentage of paraffins, cycloparaffins, and aromatics remains at 99.5%. This facilitated a comparison of the ΔG values associated with various cycloparaffin and aromatic concentrations within the SAFs.

Furthermore, when calculating SAF synthesis from CO/CO₂ through different intermediates, we calculated the thermodynamic parameters for two separate reaction stages: from CO/CO₂ hydrogenation to intermediates and from these intermediates to the final SAF products. This approach allowed us to pinpoint the most thermodynamically advantageous pathways for SAF synthesis directly from CO/CO₂.

4. Conclusions

This study offers comprehensive thermodynamic insights into the synthesis of SAF from CO/CO₂ hydrogenation. We identify temperature thresholds beyond which CO and CO₂ hydrogenation reactions become non-spontaneously feasible, constraining SAF products' direct or indirect synthesis. Moreover, we find that aromatic synthesis from CO/CO₂ hydrogenation is thermodynamically more favorable at higher temperatures. Variations in the proportion of cycloparaffin in FT-SPK and aromatic content in SPK/A significantly impact ΔG , with increasing aromatic content in SPK/A notably enhancing the driving force for the CO/CO₂ hydrogenation reaction. Among all the hydrocarbon target products, the hydrogenation synthesis process targeting aromatics not only exhibits the highest thermodynamic driving force but also has the lowest hydrogen consumption. Regarding the synthesis of SAF via specific intermediates, the study highlights several challenges, especially for hexene, ethene, and methanol synthesized from CO/CO₂ hydrogenation at higher temperatures. However, the transformation of methanol, ketene, and formaldehyde into different aviation fuels demonstrates a strong thermodynamic drive, with methanol showing minimal dependency on the reaction temperature. Overall, this research could aid in the development of more sustainable, efficient, and thermodynamically favorable strategies for green aviation fuel production.

Author Contributions: Conceptualization, C.Z. and B.L.; methodology, C.Z. and B.L.; software, B.L.; validation, B.L., Q.Z. and Z.W.; formal analysis, Q.Z., Z.W. and X.F.; investigation, B.L. and X.Y. and Y.C.; resources, F.W., C.Z. and Z.W.; data curation, B.L.; writing—original draft preparation, B.L. and Q.Z.; writing—review and editing, C.Z.; visualization, C.Z. and B.L.; supervision, F.W. and C.Z.; project administration, F.W., C.Z. and Y.C.; funding acquisition, F.W. and C.Z. All authors have read and agreed to the published version of the manuscript.

Funding: This research was funded by National Natural Science Foundation of China grant number (22278238, 22208186, and 22238004) and Beijing Nova Program (2022118).

Data Availability Statement: Not applicable.

Acknowledgments: We would like to thank the Key Research and Development Program of Inner Mongolia and Ordos, Ordos-Tsinghua Innovative & Collaborative Research Program in Carbon Neutrality, and Ordos Laboratory.

Conflicts of Interest: The authors declare no conflict of interest.

References

1. Wang, F.; Harindintwali, J.D.; Yuan, Z.; Wang, M.; Wang, F.; Li, S.; Yin, Z.; Huang, L.; Fu, Y.; Li, L.; et al. Technologies and perspectives for achieving carbon neutrality. *Innovation* **2021**, *2*, 100180. [[CrossRef](#)] [[PubMed](#)]
2. Gonzalez-Garay, A.; Heuberger-Austin, C.; Fu, X.; Klokkenburg, M.; Zhang, D.; van der Made, A.; Shah, N. Unravelling the potential of sustainable aviation fuels to decarbonise the aviation sector. *Energy Environ. Sci.* **2022**, *15*, 3291–3309. [[CrossRef](#)]
3. Zhang, H.; Fang, Y.; Wang, M.; Appels, L.; Deng, Y. Prospects and perspectives foster enhanced research on bio-aviation fuels. *J. Environ. Manag.* **2020**, *274*, 111214. [[CrossRef](#)] [[PubMed](#)]
4. Freire, M.; Kosova, N.V.; Jordy, C.; Chateigner, D.; Lebedev, O.I.; Maignan, A.; Pralong, V. A new active Li-Mn-O compound for high energy density Li-ion batteries. *Nat. Mater.* **2016**, *15*, 173–177. [[CrossRef](#)]
5. Kumabe, K.; Sato, T.; Matsumoto, K.; Ishida, Y.; Hasegawa, T. Production of hydrocarbons in Fischer–Tropsch synthesis with Fe-based catalyst: Investigations of primary kerosene yield and carbon mass balance. *Fuel* **2010**, *89*, 2088–2095. [[CrossRef](#)]
6. Akter, H.A.; Dwivedi, P.; Masum, M.F.H.; Alam, A.; Anderson, W. Does Intercropping Carinata with Loblolly Pine for Sustainable Aviation Fuel Production Save Carbon? A Case Study from the Southern United States. *BioEnergy Res.* **2022**, *15*, 1427–1438. [[CrossRef](#)]
7. Regalbuto, J. An NSF perspective on next generation hydrocarbon biorefineries. *Comput. Chem. Eng.* **2010**, *34*, 1393–1396. [[CrossRef](#)]
8. Perego, C.; Bortolo, R.; Zennaro, R. Gas to liquids technologies for natural gas reserves valorization: The Eni experience. *Catal. Today* **2009**, *142*, 9–16. [[CrossRef](#)]
9. Rahmes, T.; Kinder, J.; Crenfeldt, G.; LeDuc, G.; Abe, Y.; McCall, M.; Henry, T.; Zombanakis, G.; Lambert, D.; Lewis, C.; et al. Sustainable Bio-Derived Synthetic Paraffinic Kerosene (Bio-SPK) Jet Fuel Flights and Engine Tests Program Results. In Proceedings of the 9th AIAA Aviation Technology, Integration, and Operations Conference (ATIO), Hilton Head, SC, USA, 21–23 September 2009.
10. Jayarathna, L.; Kent, G.; O'Hara, I.; Hobson, P. A Geographical Information System based framework to identify optimal location and size of biomass energy plants using single or multiple biomass types. *Appl. Energy* **2020**, *275*, 115398. [[CrossRef](#)]

11. Wang, G.; Zhang, J.; Shao, J.; Ren, S. Characterisation and model fitting kinetic analysis of coal/biomass co-combustion. *Thermochim. Acta* **2014**, *591*, 68–74. [[CrossRef](#)]
12. Shu, Y.M.; Shi, C.X.; Pan, L.; Zhang, X.W.; Zou, J.J. Progressing production and application of biomass-based jet fuel. *Pet. Process. Petrochem.* **2021**, *52*, 88–93.
13. Holladay, J.; Abdullah, Z.; Heyne, J. *Sustainable Aviation Fuel: Review of Technical Pathways*; US Department of Energy: Washington, WA, USA, 2020; p. 81.
14. Ni, M.; Leung, D.Y.C.; Leung, M.K.H.; Sumathy, K. An overview of hydrogen production from biomass. *Fuel Process. Technol.* **2006**, *87*, 461–472. [[CrossRef](#)]
15. Janke, C.; Duyar, M.S.; Hoskins, M.; Farrauto, R. Catalytic and adsorption studies for the hydrogenation of CO₂ to methane. *Appl. Catal. B Environ.* **2014**, *152*, 184–191. [[CrossRef](#)]
16. Fan, W.K.; Tahir, M. Recent trends in developments of active metals and heterogenous materials for catalytic CO₂ hydrogenation to renewable methane: A review. *J. Environ. Chem. Eng.* **2021**, *9*, 105460. [[CrossRef](#)]
17. Su, X.; Xu, J.; Liang, B.; Duan, H.; Hou, B.; Huang, Y. Catalytic carbon dioxide hydrogenation to methane: A review of recent studies. *J. Energy Chem.* **2016**, *25*, 553–565. [[CrossRef](#)]
18. Bowker, M. Methanol Synthesis from CO₂ Hydrogenation. *ChemCatChem* **2019**, *11*, 4238–4246. [[CrossRef](#)]
19. Onishi, N.; Himeda, Y. Homogeneous catalysts for CO₂ hydrogenation to methanol and methanol dehydrogenation to hydrogen generation. *Coord. Chem. Rev.* **2022**, *472*, 214767. [[CrossRef](#)]
20. Chiang, C.-L.; Lin, K.-S.; Chuang, H.-W. Direct synthesis of formic acid via CO₂ hydrogenation over Cu/ZnO/Al₂O₃ catalyst. *J. Clean. Prod.* **2018**, *172*, 1957–1977. [[CrossRef](#)]
21. Masuda, S.; Mori, K.; Kuwahara, Y.; Louis, C.; Yamashita, H. Additive-Free Aqueous Phase Synthesis of Formic Acid by Direct CO₂ Hydrogenation over a PdAg Catalyst on a Hydrophilic N-Doped Polymer–Silica Composite Support with High CO₂ Affinity. *ACS Appl. Energy Mater.* **2020**, *3*, 5847–5855. [[CrossRef](#)]
22. Ren, S.; Shoemaker, W.R.; Wang, X.; Shang, Z.; Klinghoffer, N.; Li, S.; Yu, M.; He, X.; White, T.A.; Liang, X. Highly active and selective Cu-ZnO based catalyst for methanol and dimethyl ether synthesis via CO₂ hydrogenation. *Fuel* **2019**, *239*, 1125–1133. [[CrossRef](#)]
23. Şeker, B.; Dizaji, A.K.; Balci, V.; Uzun, A. MCM-41-supported tungstophosphoric acid as an acid function for dimethyl ether synthesis from CO₂ hydrogenation. *Renew. Energy* **2021**, *171*, 47–57. [[CrossRef](#)]
24. Ma, Z.; Porosoff, M.D. Development of Tandem Catalysts for CO₂ Hydrogenation to Olefins. *ACS Catal.* **2019**, *9*, 2639–2656. [[CrossRef](#)]
25. Gao, P.; Li, S.; Bu, X.; Dang, S.; Liu, Z.; Wang, H.; Zhong, L.; Qiu, M.; Yang, C.; Cai, J.; et al. Direct conversion of CO₂ into liquid fuels with high selectivity over a bifunctional catalyst. *Nat. Chem.* **2017**, *9*, 1019–1024. [[CrossRef](#)]
26. Ahmad, K.; Upadhyayula, S. Greenhouse gas CO₂ hydrogenation to fuels: A thermodynamic analysis. *Environ. Prog. Sustain. Energy* **2019**, *38*, 98–111. [[CrossRef](#)]
27. Claeys, M. Cobalt gets in shape. *Nature* **2016**, *538*, 44–45. [[CrossRef](#)] [[PubMed](#)]
28. Zhu, M.; Ge, Q.; Zhu, X. Catalytic Reduction of CO₂ to CO via Reverse Water Gas Shift Reaction: Recent Advances in the Design of Active and Selective Supported Metal Catalysts. *Trans. Tianjin Univ.* **2020**, *26*, 172–187. [[CrossRef](#)]
29. Chang, C.D.; Lang, W.H.; Silvestri, A.J. Synthesis gas conversion to aromatic hydrocarbons. *J. Catal.* **1979**, *56*, 268–273. [[CrossRef](#)]
30. Tian, G.; Liang, X.; Xiong, H.; Zhang, C.; Wei, F. A perspective of CO_x conversion to aromatics. *EES Catal.* **2023**, *1*, 677–686. [[CrossRef](#)]
31. Tian, G.; Liu, X.; Zhang, C.; Fan, X.; Xiong, H.; Chen, X.; Li, Z.; Yan, B.; Zhang, L.; Wang, N.; et al. Accelerating syngas-to-aromatic conversion via spontaneously monodispersed Fe in ZnCr₂O₄ spinel. *Nat. Commun.* **2022**, *13*, 5567. [[CrossRef](#)]
32. Cheng, K.; Zhou, W.; Kang, J.; He, S.; Shi, S.; Zhang, Q.; Pan, Y.; Wen, W.; Wang, Y. Bifunctional Catalysts for One-Step Conversion of Syngas into Aromatics with Excellent Selectivity and Stability. *Chem* **2017**, *3*, 334–347. [[CrossRef](#)]
33. Yan, Q.; Lu, Y.; Wan, C.; Han, J.; Rodriguez, J.; Yin, J.J.; Yu, F. Synthesis of Aromatic-Rich Gasoline-Range Hydrocarbons from Biomass-Derived Syngas over a Pd-Promoted Fe/HZSM-5 Catalyst. *Energy Fuels* **2014**, *28*, 2027–2034. [[CrossRef](#)]
34. Yang, J.; Pan, X.; Jiao, F.; Li, J.; Bao, X. Direct conversion of syngas to aromatics. *Chem. Commun.* **2017**, *53*, 11146–11149. [[CrossRef](#)]
35. Ni, Y.; Chen, Z.; Fu, Y.; Liu, Y.; Zhu, W.; Liu, Z. Selective conversion of CO₂ and H₂ into aromatics. *Nat. Commun.* **2018**, *9*, 3457. [[CrossRef](#)]
36. Xu, Y.; Liu, D.; Liu, X. Conversion of syngas toward aromatics over hybrid Fe-based Fischer-Tropsch catalysts and HZSM-5 zeolites. *Appl. Catal. A Gen.* **2018**, *552*, 168–183. [[CrossRef](#)]
37. Sun, Q.; Wang, N.; Yu, J. Advances in Catalytic Applications of Zeolite-Supported Metal Catalysts. *Adv. Mater.* **2021**, *33*, e2104442. [[CrossRef](#)]
38. Yang, X.; Su, X.; Liang, B.; Zhang, Y.; Duan, H.; Ma, J.; Huang, Y.; Zhang, T. The influence of alkali-treated zeolite on the oxide-zeolite syngas conversion process. *Catal. Sci. Technol.* **2018**, *8*, 4338–4348. [[CrossRef](#)]
39. Arslan, M.T.; Ali, B.; Gilani, S.Z.A.; Hou, Y.; Wang, Q.; Cai, D.; Wang, Y.; Wei, F. Selective Conversion of Syngas into Tetramethylbenzene via an Aldol-Aromatic Mechanism. *ACS Catal.* **2020**, *10*, 2477–2488. [[CrossRef](#)]
40. Wang, J.; Li, G.; Li, Z.; Tang, C.; Feng, Z.; An, H.; Liu, H.; Liu, T.; Li, C. A highly selective and stable ZnO-ZrO₂ solid solution catalyst for CO₂ hydrogenation to methanol. *Sci. Adv.* **2017**, *3*, e1701290. [[CrossRef](#)]
41. Xu, Y.; Liu, J.; Ma, G.; Wang, J.; Wang, Q.; Lin, J.; Wang, H.; Zhang, C.; Ding, M. Synthesis of aromatics from syngas over FeMnK/SiO₂ and HZSM-5 tandem catalysts. *Mol. Catal.* **2018**, *454*, 104–113. [[CrossRef](#)]
42. Cheng, L.; Meng, C.; Yang, T.; Li, N.; Liu, D. One-Step Synthesis of Aromatics from Syngas over K-Modified FeMnO/MoNi-ZSM-5. *Energy Fuels* **2018**, *32*, 9756–9762. [[CrossRef](#)]

43. Wang, T.; Xu, Y.; Shi, C.; Jiang, F.; Liu, B.; Liu, X. Direct production of aromatics from syngas over a hybrid FeMn Fischer–Tropsch catalyst and HZSM-5 zeolite: Local environment effect and mechanism-directed tuning of the aromatic selectivity. *Catal. Sci. Technol.* **2019**, *9*, 3933–3946. [[CrossRef](#)]
44. Wang, S.; Fang, Y.; Huang, Z.; Xu, H.; Shen, W. The Effects of the Crystalline Phase of Zirconia on C–O Activation and C–C Coupling in Converting Syngas into Aromatics. *Catalysts* **2020**, *10*, 262. [[CrossRef](#)]
45. Li, Z.; Qu, Y.; Wang, J.; Liu, H.; Li, M.; Miao, S.; Li, C. Highly Selective Conversion of Carbon Dioxide to Aromatics over Tandem Catalysts. *Joule* **2019**, *3*, 570–583. [[CrossRef](#)]
46. Zhou, C.; Shi, J.; Zhou, W.; Cheng, K.; Zhang, Q.; Kang, J.; Wang, Y. Highly Active ZnO–ZrO₂ Aerogels Integrated with H-ZSM-5 for Aromatics Synthesis from Carbon Dioxide. *ACS Catal.* **2019**, *10*, 302–310. [[CrossRef](#)]
47. Wang, Y.; Kazumi, S.; Gao, W.; Gao, X.; Li, H.; Guo, X.; Yoneyama, Y.; Yang, G.; Tsubaki, N. Direct conversion of CO₂ to aromatics with high yield via a modified Fischer–Tropsch synthesis pathway. *Appl. Catal. B Environ.* **2020**, *269*, 118792. [[CrossRef](#)]
48. Arslan, M.T.; Tian, G.; Ali, B.; Zhang, C.; Xiong, H.; Li, Z.; Luo, L.; Chen, X.; Wei, F. Highly Selective Conversion of CO₂ or CO into Precursors for Kerosene-Based Aviation Fuel via an Aldol–Aromatic Mechanism. *ACS Catal.* **2022**, *12*, 2023–2033. [[CrossRef](#)]
49. Xu, Y.; Shi, C.; Liu, B.; Wang, T.; Zheng, J.; Li, W.; Liu, D.; Liu, X. Selective production of aromatics from CO₂. *Catal. Sci. Technol.* **2019**, *9*, 593–610. [[CrossRef](#)]
50. Kasipandi, S.; Bae, J.W. Recent Advances in Direct Synthesis of Value-Added Aromatic Chemicals from Syngas by Cascade Reactions over Bifunctional Catalysts. *Adv. Mater.* **2019**, *31*, e1803390. [[CrossRef](#)]
51. Timko, M.T.; Herndon, S.C.; De La Rosa Blanco, E.; Wood, E.C.; Yu, Z.; Miake-Lye, R.C.; Knighton, W.B.; Shafer, L.; DeWitt, M.J.; Corporan, E. Combustion Products of Petroleum Jet Fuel, a Fischer–Tropsch Synthetic Fuel, and a Biomass Fatty Acid Methyl Ester Fuel for a Gas Turbine Engine. *Combust. Sci. Technol.* **2011**, *183*, 1039–1068. [[CrossRef](#)]
52. Jia, T.; Zhang, X.; Liu, Y.; Gong, S.; Deng, C.; Pan, L.; Zou, J.J. A comprehensive review of the thermal oxidation stability of jet fuels. *Chem. Eng. Sci.* **2021**, *229*, 116157. [[CrossRef](#)]
53. Tian, G.; Zhang, C.; Wei, F. CO_x conversion to aromatics: A mini-review of nanoscale performance. *Nanoscale Horiz.* **2022**, *7*, 1478–1487. [[CrossRef](#)] [[PubMed](#)]
54. Shen, X.; Kang, J.; Niu, W.; Wang, M.; Zhang, Q.; Wang, Y. Impact of hierarchical pore structure on the catalytic performances of MFI zeolites modified by ZnO for the conversion of methanol to aromatics. *Catal. Sci. Technol.* **2017**, *7*, 3598–3612. [[CrossRef](#)]
55. Zhu, J.; Su, Y.; Chai, J.; Muravev, V.; Kosinov, N.; Hensen, E.J.M. Mechanism and Nature of Active Sites for Methanol Synthesis from CO/CO₂ on Cu/CeO₂. *ACS Catal.* **2020**, *10*, 11532–11544. [[CrossRef](#)]
56. Xie, C.; Niu, Z.; Kim, D.; Li, M.; Yang, P. Surface and Interface Control in Nanoparticle Catalysis. *Chem. Rev.* **2020**, *120*, 1184–1249. [[CrossRef](#)] [[PubMed](#)]
57. Arslan, M.T.; Qureshi, B.A.; Gilani, S.A.; Cai, D.; Ma, Y.; Usman, M.; Chen, X.; Wang, Y.; Wei, F. Single-Step Conversion of H₂-Deficient Syngas into High Yield of Tetramethylbenzene. *ACS Catal.* **2019**, *9*, 2203–2212. [[CrossRef](#)]

Disclaimer/Publisher’s Note: The statements, opinions and data contained in all publications are solely those of the individual author(s) and contributor(s) and not of MDPI and/or the editor(s). MDPI and/or the editor(s) disclaim responsibility for any injury to people or property resulting from any ideas, methods, instructions or products referred to in the content.